# 10

# Mechanisms that Produce Auroral Asymmetries in Conjugate Hemispheres

**Nikolai Østgaard,[1] Jone Peter Reistad,[1] Paul Tenfjord,[1] Karl Magnus Laundal,[1] Kristian Snekvik,[1] Steve Milan,[1,2] and Stein Haaland[1,3]**

## ABSTRACT

Auroral studies have shown that there are systematic displacements and significant intensity differences of the aurora in the two hemispheres. Such observations have been systematically correlated with the various components of the interplanetary magnetic field (IMF) and hemispherical differences in solar exposure. To explain asymmetric aurora both in locations and intensities, three mechanisms have been suggested:

1. difference in region 1 currents due to hemispheric differences in the solar wind dynamo efficiency when the IMF has a significant $B_x$ component,
2. interhemispheric or asymmetric currents associated with the "penetration" of the IMF $B_y$ component into the closed magnetosphere, and
3. interhemispheric currents due to conductivity differences in the two hemispheres.

In this chapter we will discuss these mechanisms and present some recent and new results from investigating their relevance and importance. The effect of IMF $B_x$ has been found to be statistically significant in the vicinity of upward region 1 current in the dusk sector. We present a modified view of how IMF $B_y$ induces a $B_y$ component in the closed magnetosphere and how the induced magnetic stress may produce hemispherical asymmetric currents. We present statistical results of Birkeland currents that do not support the existence of strong interhemispheric currents at the sunlight terminator.

## 10.1. INTRODUCTION

The interaction between the interplanetary magnetic field (IMF) and solar wind plasma with Earth's magnetic field has been extensively studied by measuring and analyzing the auroral footpoints in the polar regions. Although most of the ground-based data are from the northern hemisphere, conjugate studies, comparing data from the southern and northern polar regions, date back to the 1960s [e.g., *Hargreaves and Chivers*, 1964; *Belon et al.*, 1969]. To avoid the limitations imposed by clouds and sunlight, conjugate aircraft flights equipped with all-sky cameras were undertaken in the late 1960s [*Stenbaek-Nielsen et al.*, 1972, 1973]. Furthermore, using spacecraft carrying global imaging instruments, it has been possible to study both polar regions extensively and in much more detail. We have now learned that the two hemispheres do not always respond similarly to solar wind forcing and magnetospheric processes, and also that the different solar exposures play an important role in producing asymmetric behavior in the two hemispheres.

Hemispherical asymmetry in the behavior of the dayside aurora and currents has been well documented [e.g., *Sandholt et al.*, 1998; *Sandholt and Farrugia*, 1999;

[1]*Birkeland Centre for Space Science, Department of Physics and Technology, University of Bergen, Bergen, Norway*

[2]*Department of Physics and Astronomy, University of Leicester, Leicester, England, UK*

[3]*Max-Planck Institute, Göttingen, Germany*

*Auroral Dynamics and Space Weather, Geophysical Monograph 215*, First Edition.
Edited by Yongliang Zhang and Larry J. Paxton.

*Zhou et al*., 2000; *Bobra et al*., 2004; *Østgaard et al*., 2005a; *Wing et al*., 2010], but in this chapter we will mostly review nightside phenomena. Most studies have focused on either systematic displacement of auroras or differences in auroral intensities in the two hemispheres. Displacements have been seen both in latitude [*Stenbaek-Nielsen and Otto*, 1997; *Laundal et al*., 2010a,b] and longitude [*Sato et al*., 1986; *Stenbaek-Nielsen and Otto*, 1997; *Sato et al*., 1998; *Frank and Sigwarth*, 2003; *Burns et al*., 1990; *Liou et al*., 2001b; *Liou and Newell* , 2010; *Wang et al*., 2007; *Østgaard et al*., 2004, 2005b; *Motoba et al*., 2010; *Østgaard et al*., 2011a,b]. These displacements have been attributed to asymmetric currents or directly to IMF influence on the magnetic configuration of the closed magnetosphere [*Stenbaek-Nielsen and Otto*, 1997; *Vorobjev et al*., 2001; *Wang et al*., 2007; *Liou et al*., 2001b; *Liou and Newell* , 2010; *Østgaard et al*., 2004, 2005b; *Laundal and Østgaard*, 2009; *Østgaard et al*., 2011a,b]. Several papers have explained the observed auroral intensity differences by field-aligned currents (FACs) due to differences in ionospheric conductivity [*Stenbaek-Nielsen et al*., 1972; *Newell et al*., 1996; *Sato et al*., 1998; *Liou et al*., 2001a; *Meng et al*., 2001; *Newell et al*., 2010]. Statistical studies using global Polar Ultraviolet Imager (UVI) data have also shown significant differences in the nightside auroral brightness in the Northern Hemisphere due to IMF $B_y$ polarity [*Shue et al*., 2001] and a smaller but still statistical significant intensity asymmetry due to IMF $B_x$ polarity [*Shue et al*., 2002]. The first report from simultaneous global imaging from space revealed that the theta aurora could be a conjugate phenomenon [*Craven et al*., 1991]. However, it was shown later, using simultaneous data from Polar VIS Earth camera [*Frank et al*., 1995] and the IMAGE-FUV instruments [*Mende et al*., 2000] that theta aurora could also be a non-conjugate phenomenon [*Østgaard et al*., 2003].

Earlier reviews of conjugate auroral studies can be found in *Østgaard et al*. [2007] and *Østgaard and Laundal* [2012]. In the latter we summarized our findings combined with earlier theoretical studies and suggested three mechanisms that can produce interhemispheric or asymmetric currents and different auroral brightness in the two hemispheres. They will be described in the next three subsections.

### 10.1.1. Difference in Region 1 Currents Due to Hemispheric Differences in Solar Wind Dynamo Efficiency When IMF Has a Significant $B_x$ Component

According to the open magnetospheric model [*Dungey*, 1961], magnetic flux is opened on the dayside and closed on the nightside. As the opened magnetic flux tubes are draped down the tail, the tension force on these flux tubes tends to slow them down, and as first noticed by *Cowley* [1981b], the orientation of the IMF in the *XZ* plane (in CGM or GSE coordinate system) would lead to different strength of the tension force in the two hemispheres, as shown in Figure 10.1a. This tension force gives rise to a current generator and as part of these currents close in the ionosphere (Figure 10.1b) interhemispheric differences in auroral brightness should be seen in the dusk sector, assuming that the current carriers are precipitating electrons. *Laundal and Østgaard* [2009] reported a significantly brighter aurora in the southern dusk that lasted for more than an hour. With a $B_x > 0$ dominant IMF, this observation is consistent with this mechanism. Another support for this mechanism can be found in *Shue et al*. [2002] that reported an overall brighter aurora in the Northern Hemisphere for IMF $B_x < 0$.

### 10.1.2. Interhemispheric or Asymmetric Currents Associated with "Penetration" of IMF $B_y$ Component into Closed Magnetosphere

As pointed out earlier in this section, many studies have reported longitudinal displacement of auroras between the two hemispheres. Furthermore, they have shown that this displacement is strongly correlated with IMF clock angle and IMF $B_y$. This is strong evidence that IMF $B_y$ is accompanied with a $B_y$ component in the closed magnetosphere and creates asymmetric magnetic footpoints and a twisted magnetic field configuration from one hemisphere to the other. *Østgaard and Laundal* [2012] referred to the explanation suggested by *Stenbaek-Nielsen and Otto* [1997], which is shown in Figure 10.1c and is often regarded as a penetration of IMF $B_y$ into the closed magnetosphere. Although this description is consistent with observations of nonconjugate aurora from a conjugate aircraft campaign [*Stenbaek-Nielsen and Otto*, 1997], it does not provide a detailed description of how the asymmetric stresses in the tail can propagate from the common generator region in the equatorial plane to the ionosphere(s). In Section 10.2.3 we will suggest a modified scenario where IMF $B_y$ does *not* penetrate but induces a $B_y$ component in the closed magnetosphere. We will also argue that the result is *not* an interhemispheric current, but an asymmetric current from the plasma sheet into the two hemispheres.

### 10.1.3. Interhemispheric Currents Due to Conductivity Differences in the Two Hemispheres

*Richmond and Roble* [1987] modeled interhemispheric currents at middle and low latitudes produced by thermospheric winds. The existence of such currents has been supported by observations [*Olsen*, 1997]. It has also been suggested that interhemispheric currents should

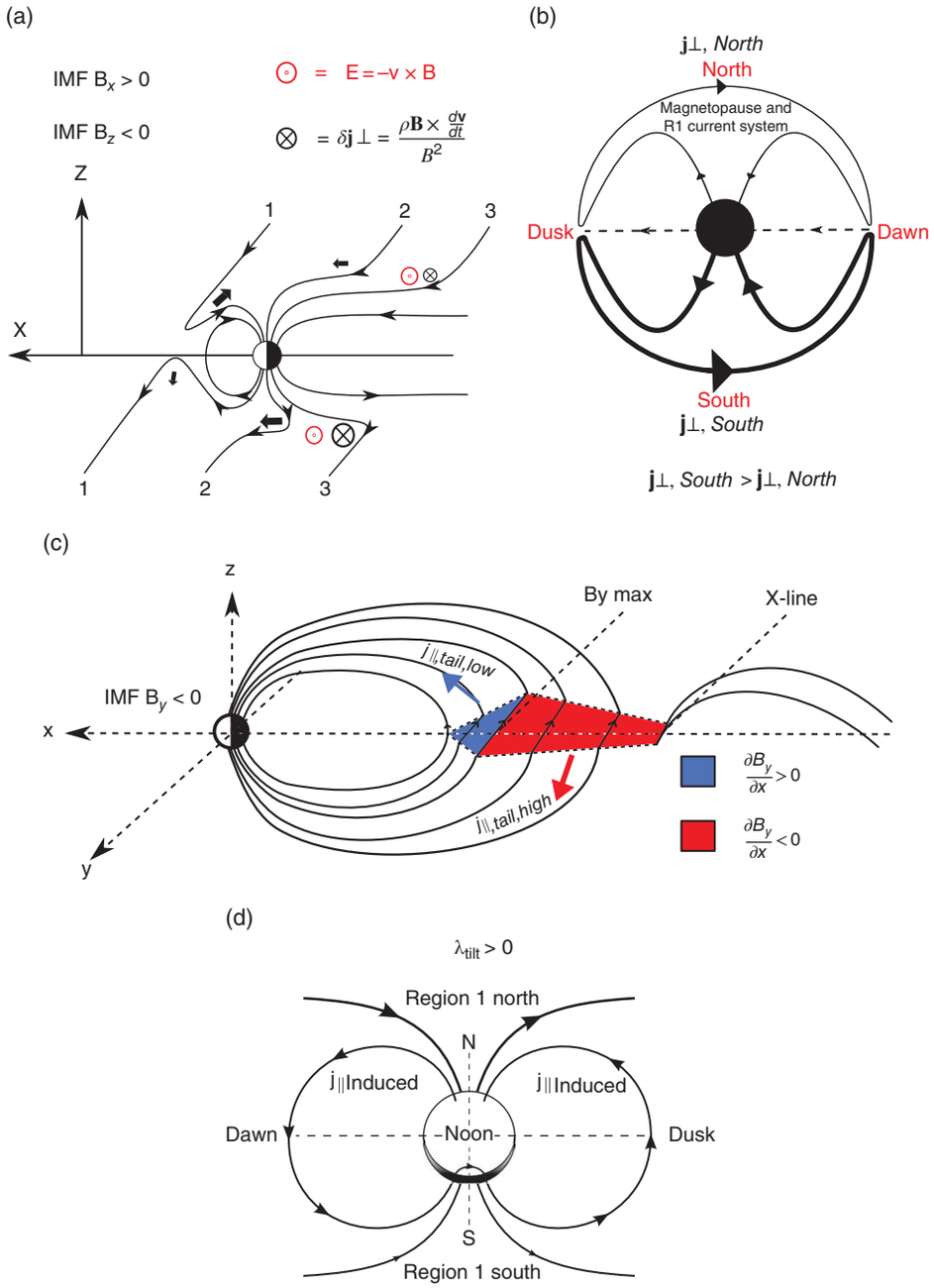


**Figure 10.1** The three suggested mechanisms for nonconjugate aurora: (a) due to a positive IMF $B_x$ (and $B_z < 0$) the magnetic tension force on open field lines (2 and 3) is larger in the Southern Hemisphere (black large arrows) than in the Northern Hemisphere (after *Cowley* [1981b], Figure 2); (b) associated current systems; (c) penetration of IMF $B_y < 0$ into the closed magnetosphere showing the pileup region (after *Stenbaek-Nielsen and Otto* [1997], Figure 4); (d) Induced interhemispheric currents due to conductivity differences in the conjugate regions for dipole tilt $\lambda_{tilt} > 0$ (after *Benkevich et al*. [2000], Figure 1). This figure is similar to Figure 2 in *Reistad et al*. [2013].

exist at high latitudes in the vicinity of the terminator, but such currents have so far not been supported by direct observations. *Benkevich et al*. [2000] modeled the redistribution of the three-dimensional current system due to different ionospheric conductivity in the dark and sunlit conjugate hemispheres and suggested that an interhemispheric current component can be established. According to *Benkevich et al*. [2000], the high-latitude currents (region 1), due to the low conductivity in the dark hemisphere, are weak and cannot close in that hemisphere, but

as the two hemispheres are connected by highly conductive magnetic field lines, currents can flow out of the sunlit hemisphere into the region of the large conductivity gradient in the dark hemisphere near the terminator and close through the sunlit part of that hemisphere, as schematically shown in Figure 10.1d. *Laundal and Østgaard* [2009] speculated that the transient spot seen only in the Northern Hemisphere that they reported could be a signature of this mechanism. The strength of these currents is postulated to maximize for large tilt angles, and there are claims from modeling efforts that they constitute a significant part of the global FAC system [*Lyatskaya et al.*, 2014]. In Section 10.2.4 we will present statistical results of Birkeland currents based on data from Active Magnetosphere and Planetary Electrodynamics Response Experiment (AMPERE). As will be seen, the results do not support the existence of interhemispheric currents with magnitudes comparable to the region 1 and 2 currents, and we will argue that the transient spot reported by *Laundal and Østgaard* [2009] was probably not caused by this mechanism.

In the following we will review some results that have explored the relevance and importance of these mechanisms.

## 10.2. RECENT RESULTS

In this section we will review some recent results of exploring the importance of these mechanisms.

### 10.2.1. A Small Statistical Study of Importance of the Three Mechanisms

*Reistad et al.* [2013] investigated 19 h of simultaneous global conjugate auroral data containing 10 sequences with duration from 1 to 5 h during active geomagnetic conditions. The imaging data were from IMAGE FUV WIC and Polar VIS Earth camera. They identified 15 features of nonconjugate aurora, meaning features that were observed in only one hemisphere or a feature that was significantly more intense in one hemisphere than the other. They developed a fairly robust scheme in order to compare intensities from the two cameras measuring two different ultraviolet wavelength bands. Figure 10.2a shows an example of the auroral images on a rectangular grid. A 2D cross-correlation algorithm, similar to that used by *Østgaard et al.* [2011b], was applied to find that the northern aurora should be shifted −1.3 magnetic local time (MLT) to match the aurora in the south. The IMF had a positive $B_x$ component and a larger negative $B_y$ component, while $B_z$ was slightly negative. The two nonconjugate features are denoted 1 and 2, where feature 1 is consistent with the (negative) IMF $B_y$ penetration mechanism and an interhemispheric current going from north to south (see Figure 10.1c, but also our revised view in Figure 10.4c) and feature 2 with the more efficient solar dynamo in the Southern Hemisphere, due to the positive IMF $B_x$ (see Figure 10.1a,b). Feature 2 is in the dusk sector and at the poleward edge as expected for upward region 1 current.

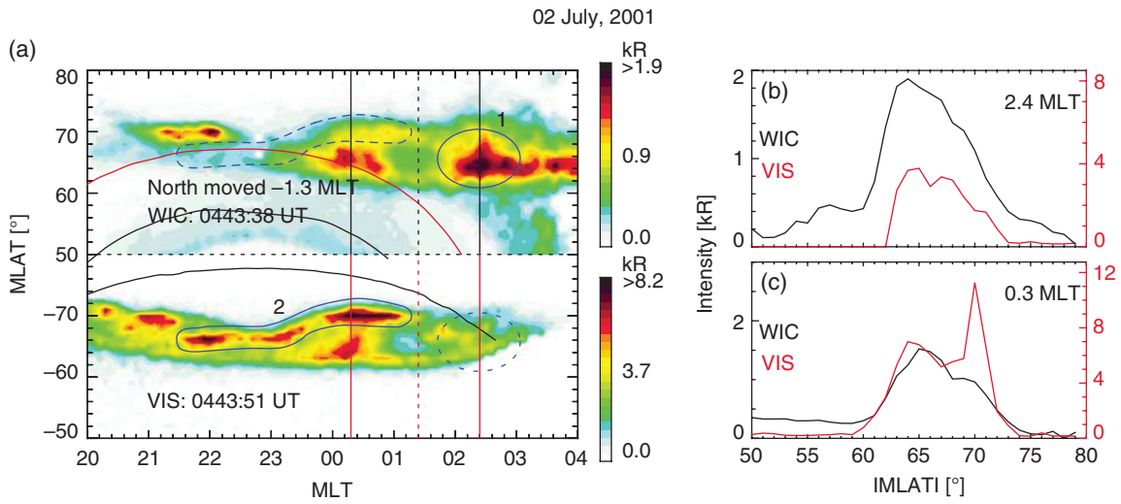


**Figure 10.2** The nonconjugate aurora on July 2, 2001. (a) The image pair mapped to a rectangular magnetic grid. The northern aurora has been longitudinally shifted by −1.3 MLT. Regions of nonconjugate aurora are indicated with solid blue rings, and the corresponding conjugate area, with dashed blue rings. The red (black) lines indicate SZA = 100° (110°). (b) Intensity profiles along 2.4 MLT of feature 1 where black line is Northern Hemisphere and red line is Southern Hemisphere. (c) Intensity profiles along 0.3 MLT of feature 2 from both hemispheres. This figure is similar to Figure 2C,D,E in *Reistad et al.* [2013].

Similar examinations were performed on all the 15 nonconjugate features and it was found that 7 features were consistent with the solar wind dynamo mechanism, 5 due to the penetration of IMF $B_y$ and 3 due to conductivity differences. In addition, 5 features could be explained by more than one mechanism. The conclusion of the *Reistad et al*. [2013] paper is that nonconjugate aurora is a common phenomenon and that most of them were consistent with a more efficient solar wind dynamo due to a significant IMF $B_x$ component.

### 10.2.2. Asymmetric Region 1 Currents Driven by Difference in Solar Wind Dynamo Efficiency Due to IMF $B_x$

Following the results from *Reistad et al*. [2013], a statistical study with a larger amount of data has been performed [*Reistad et al*., 2014] to explore whether the difference in solar wind dynamo efficiency is statistically significant. For this study the entire IMAGE FUV WIC dataset was used. Careful selection criteria were implemented to avoid the effect of other possible mechanisms: (1) |IMF $B_x$| > 2 nT, (2) |IMF $B_y$ | < 2 nT, (3) IMF $B_z$ < 0 nT, (4) 10° < |dipole tilt| < 30° (both hemispheres in darkness), (5) intervals of >10 min between observations, and (6) the five criteria must be satisfied for >10 min.

The images were separated in two groups, one for IMF $B_x$ > 2 nT and one for IMF $B_x$ < −2 nT. Before the images were added together, they were transformed into a common 10-bin latitudinal grid defined by the polar and equatorward boundaries of the aurora. The results are shown in Figure 10.3. In the Northern Hemisphere the superposed images (Figure 10.3a,b) include >150 observations in the MLT sector from 17 to 24, while for the Southern Hemisphere images (Figure 10.3d,e) there are >80 observations in the same MLT sector. As can be seen in Figure 10.3c,f, there are distinct intensity differences between the negative and

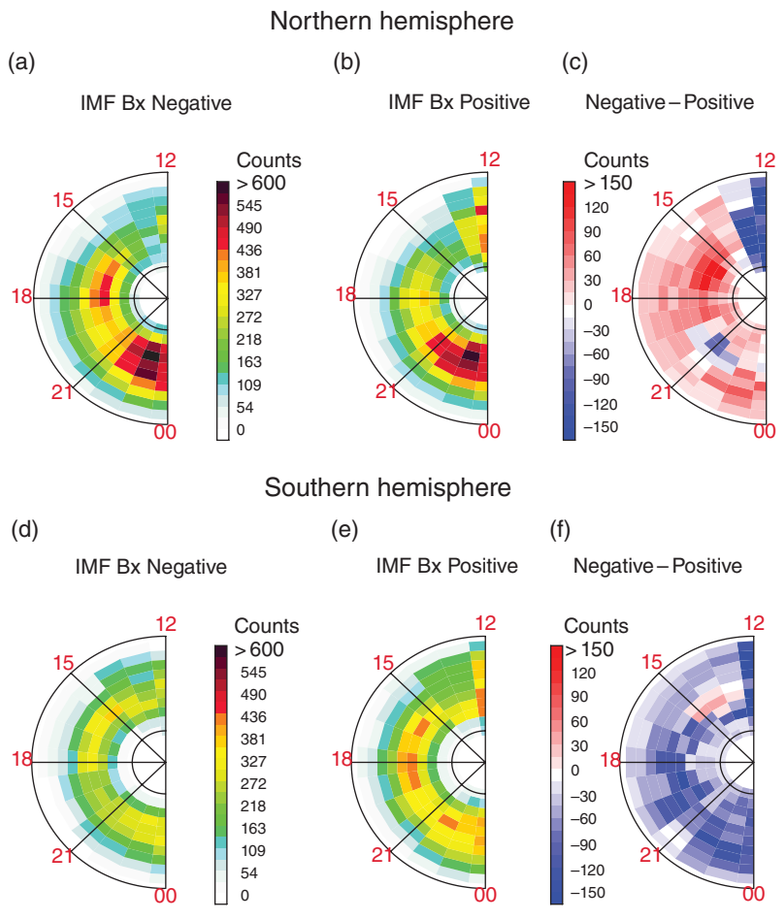


**Figure 10.3** Superposed images of auroral luminosity: (a,d) Northern and Southern Hemispheres for IMF $B_x$ negative; (b,e) Northern and Southern Hemispheres for IMF $B_x$ positive; (c,f) difference between (a), (b) and (d), (e). This figure is similar to Figure 3 and Figure 4A,B,C in *Reistad et al*. [2014].

positive IMF $B_x$ cases. The differences are seen in the dusk sector (15−19 MLT in the north and 16−20 MLT in the south) and at the poleward edge, most clearly in the Northern Hemisphere.

This is exactly as expected from the efficiency difference of the solar wind dynamo due to IMF $B_x$ component where this upward region 1 current closes in the poleward region of the ionospheric dusk sector. A Kolmogorov−Smirnov test showed that the differences are significant on a 95% confidence level within most of the indicated regions [*Reistad et al*., 2014].

### 10.2.3. Asymmetric Currents that May Arise from IMF $B_y$-Induced Stress on Closed Field Lines

As pointed out in Section 10.1.2, *Østgaard and Laundal* [2012] referred to the geometry and the explanation suggested by *Stenbaek-Nielsen and Otto* [1997] (see Figure 10.1c). This explanation considered a penetration of IMF $B_y$ into the closed magnetosphere through reconnection in the tail and that the transport of closed magnetic flux toward Earth would produce a gradient, $\frac{\partial B_y}{\partial x} \sim J_z$, in the neutral plasma sheet. Here, we propose a modified scenario where IMF $B_y$ does *not* penetrate but induces a $B_y$ component in the closed magnetosphere. We will also argue that the result is *not* an interhemispheric current, but an asymmetric current from the plasmasheet into the two hemispheres.

First, we will explain how the IMF $B_y$ will induce a $B_y$ component in the closed magnetosphere. We consider a hypothetical event in the solar wind with IMF $B_z$ negative and where IMF $B_y$ is initially zero and then jumps to a constant positive value. When IMF has a $B_y$ component, the merging with Earth's magnetic field will result in a dawn−dusk asymmetry of the open magnetic flux in the lobes in the two hemispheres. This is shown in Figure 10.4a for positive IMF $B_y$ (the same as Figure 3a in *Liou and Newell* [2010] and similar to Figure 5 in *Khurana et al*. [1996]). The added magnetic flux will be opposite in the two hemispheres, and consequently the forces acting on the field lines in the two hemispheres will be oppositely directed [*Cowley*, 1981a; *Liou and Newell*, 2010]. These magnetic pressure forces will also affect closed field lines and lead to the longitudinal asymmetry of the footpoints. The result is an induced $B_y$ component in the closed magnetosphere with the same direction as the IMF $B_y$, as seen in Figure 10.4a. This is how the IMF $B_y$ induces a $B_y$ component in the closed magnetosphere shortly after the entrance of an IMF $B_y$ component to the dayside magnetopause.

Now, we will describe the dynamics of this induced $B_y$ component. In Figure 10.4b we illustrate the anticipated situation in the midtail region for a magnetic field line with asymmetric footpoints in the two dawn cells. The situation is shown for a positive IMF $B_y$, hence the crescent "banana" convection cell is seen on the dawnside in the Northern Hemisphere (top) and on the duskside in the Southern Hemisphere (bottom).

The asymmetric pressure forces from the lobes, indicated by the $-\nabla P^t$ arrows, are now balanced by the tension forces on the field line, illustrated by the $\vec{T}$ arrows. For simplicity, the induced $B_y$ component is confined between the two black horizontal lines. In the lower part of Figure 10.4b we illustrate the current system that will be associated with the induced $B_y$ component when the forces are balanced. The view is in the $XZ$ plane, and again the $B_y$ component is confined within the area depicted by dashed lines, corresponding to the region between the horizontal black lines mentioned above. This means that there will be a step-like positive gradient in $\frac{\partial B_y}{\partial x}$ on the right side (tailward) of the box and a negative gradient on the inner side (Earthward) of the box. Ampére's law, $\frac{\partial B_y}{\partial x} \sim J_z$, this means that we have an upward current on the right side and a downward on the left side, both shown with purple arrows. The tension forces ($\vec{T}$) that balance the pressure forces ($-\nabla P^t$) require currents along $X$ as shown by the blue and red arrows in both panels of Figure 10.4b. In such a balanced situation the current system is closed locally and the stress on the field lines will not be transported away from that region.

Now, we follow this field line as it convects toward Earth (here: $X = -6R_E$). As this field line moves further inside the magnetosphere, the lobe pressure will have a weaker effect but the total pressure (magnetic and plasma) from Earth becomes larger. We illustrate this scenario in Figure 10.4c. To emphasize our point, we neglect the lobe pressure and represent the pressure gradient force from Earth by $-\nabla P_0$. For field lines with footpoints in the dawn cell, this force will be dawnward in both hemispheres (in the dusk cell it will be duskward). In the Southern Hemisphere the tension force ($\vec{T}$) and Earth pressure force ($-\nabla P_0$) are opposite but in the Northern Hemisphere they are both directed dawnward. Consequently, most of the stress is transmitted toward the Northern Ionosphere, and this will act to restore symmetry of the footpoints of the field line. The Northern Hemisphere footpoint will therefore move faster than the footpoint in the Southern Hemisphere., which is consistent with the longer trajectory that the footpoints in the "banana" cell has to travel compared to the "orange" cell in order to reach symmetry. The final situation is shown in Figure 10.4d.

As the stress propagates mostly into the northern ionosphere from the situation in panels (c) to (d), it represents a field-aligned current going from the equatorial plane to the northern ionosphere. This propagation is illustrated in the lower part in Figure 10.4c. However, this

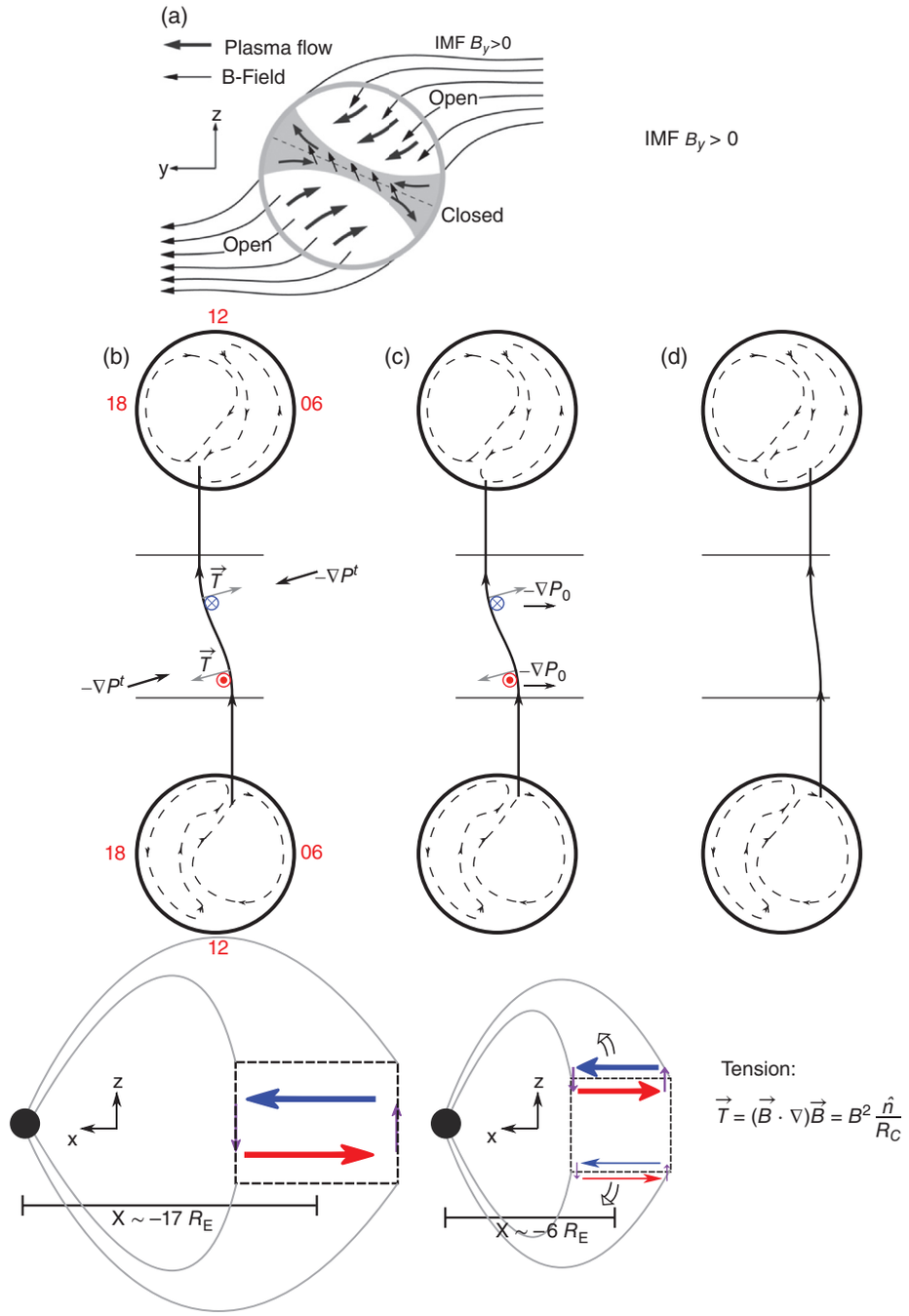


**Figure 10.4** (a) Asymmetric entry of magnetic flux in the lobes during positive IMF $B_y$ conditions. This panel is the same as Figure 3a in *Liou and Newell* [2010]. (b–d) A flux tube on closed field lines with asymmetric footpoints in the dawn convection cell during IMF $B_y$-positive conditions. Upper panels show pressure, tension, and asymmetric footpoints into the dawn cells. Lower panels show the associated current systems seen from dusk. (b) Just after reconnection, showing the asymmetric pressure forces due to IMF $B_y$ and the magnetic tension forces on the flux tube balance. Currents close locally as indicated in the lower panel. (c) Flux tube moves Earthward and is affected by the (total) pressure.

is not an interhemispheric current, but an asymmetric current. Furthermore, we would expect to see the signature post midnight in the Northern Hemisphere in the "banana" cell. If we had considered a flux tube convecting Earthward on the dusk cell and using the same argument, we would expect the stress and the field-aligned current to be transmitted primarily to the southern ionosphere, also the "banana" cell. Although not interhemispheric, the directions of these currents are similar as *Stenbaek-Nielsen and Otto* [1997] suggested.

Three important distinctions can be made from this scenario: (1) IMF $B_y$ does *not* penetrate the magnetosphere, but through asymmetric lobe pressure it induces a $B_y$ component with same sign as IMF $B_y$ in the closed magnetosphere; (2) the currents are *not* interhemispheric, but rather asymmetric from the plasma sheet into the two hemispheres; and (3) to establish asymmetric footpoints, we do not need to consider the Dungey cycle with nightside reconnection (assumed by, e.g., *Stenbaek-Nielsen and Otto* [1997] and *Østgaard et al*. [2004]), which will be on timescale of an hour, but just the buildup of lobe pressure, which is on a shorter timescale. In this context, the role of reconnection is to convect the field lines Earthward (return flow).

A more comprehensive explanation, model results, and interpretation on how this IMF $B_y$-induced scenario works can be found in *Tenfjord et al*. [2015].

### 10.2.4. Interhemispheric Currents Due to Conductivity Differences in the Two Hemispheres

More recent studies [*Benkevich et al*., 2000; *Lyatskaya et al*., 2014] have reported modeling results that show field-aligned currents flowing between the hemispheres at high latitudes. These results are based on the Maxwell's equations in the static case, the ionospheric Ohm's law, and the assumption that the electric potential maps perfectly between the hemispheres on closed field lines. Further, an ionospheric conductance pattern was assumed, as well as boundary conditions for the electric potential. *Benkevich et al*. [2000] used only sunlight-induced conductance in their model, while *Lyatskaya et al*. [2014] included a contribution from a typical auroral oval. The modeled interhemispheric FACs close the primary [region 1 (R1)] FAC through the opposite hemisphere, depending on the conductance differences between hemispheres, leaving or entering the ionosphere where gradients in the conductance are present.

Only indirect evidence of such currents exist [*Lyatskaya et al*., 2008; *Laundal and Østgaard*, 2009]. Direct evidence is difficult to obtain, because the interhemispheric currents are predicted to largely coincide with the traditional current systems, and may appear as either an enforcement or a reduction of such currents. However, it is known that the traditional current system can be imbalanced between the two the hemispheres, for example, when the ionospheric conductance is different [*Ohtani et al*., 2005]. We will term these as *asymmetric currents*. As these asymmetric currents can flow into the ionosphere very close to where the interhemispheric currents were predicted by *Lyatskaya et al*. [2014] and *Benkevich et al*. [2000], it can be difficult to distinguish between the two.

Here we address one of the key properties of this type of interhemispheric current, namely, that they connect to conductance gradients. Using AMPERE data, we calculate global maps of median current densities with the position of the sunlight terminator held fixed. *Benkevich et al*. [2000] predicted that the interhemispheric currents at the terminator are comparable to the R1 current, and thus we expect that they would be visible in the AMPERE maps as a perturbation to the existing current system. We focus on the conductance gradient at the terminator, since its location is much more predictable than the generally sharper gradients associated with particle precipitation.

The results are shown in Figure 10.5. The location of the sunlight terminator is confined within the red lines in each plot labeled (a)−(h). In addition, we require negative IMF $B_z$ to ensure sufficiently strong R1 currents. We also require a stable current pattern, using the mean relative overlap defined by *Anderson et al*. [2008], which we calculate on the basis of patterns 20 min apart, and require to be greater than 0.45. The number of AMPERE current maps in each plot is indicated in the lower left corners. Below the average AMPERE maps, we show the mean R1 current as a function of hour angle from the midnight meridian. The R1 current in this case is defined as the mean upward current at dusk MLT sectors and mean downward current at dawn. Each plot corresponds to the AMPERE maps labeled by the same letter. The vertical bars show where the terminator crosses the peak R1 current.

The AMPERE maps show that the Birkeland currents increase with solar illumination everywhere except in the premidnight region. This variation is similar to what was reported by *Ohtani et al*. [2005] and *Green et al*. [2009]. This behavior is consistent with the Birkeland currents scaling with the conductance, produced primarily by sunlight except premidnight, where particle precipitation dominates. The particle precipitation in this region is stronger in darkness on average [*Newell et al*., 2010].

An expected signature from interhemispheric currents would be a localized perturbation, close to the terminator. No consistent perturbation is seen in Figure 10.5. From this we conclude that any interhemispheric currents of the kind proposed by *Benkevich et al*. [2000] must be weaker than what their computations show. It is therefore not likely that such currents, at least those associated with

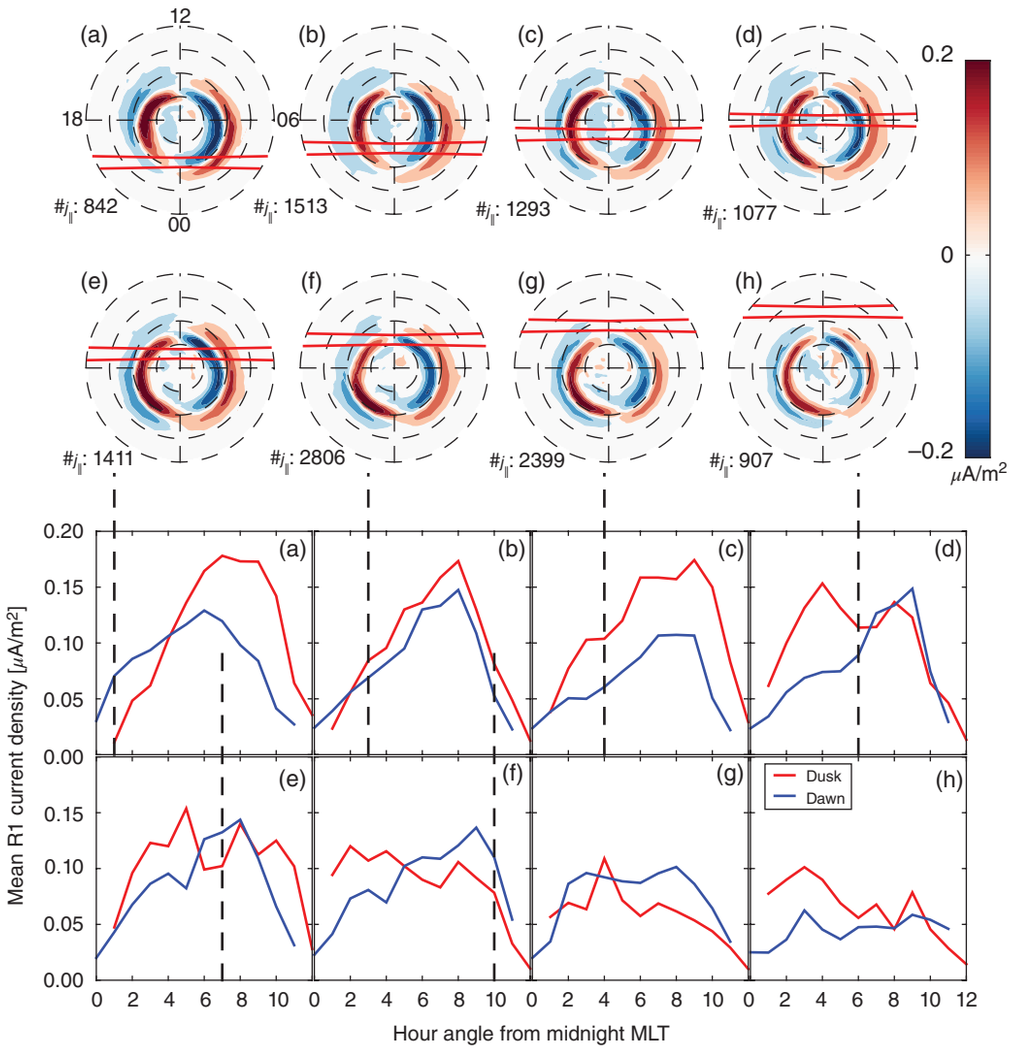


**Figure 10.5** Top: median Birkeland current densities from AMPERE, for IMF $B_z < 0$ nT, with mean relative overlap (see *Anderson et al*. [2008]) at 20-min cadence greater than 0.45. Each map is based on global Birkeland current patterns recorded when the sunlight terminator was located between the red lines. Bottom: Mean R1 current density as a function of magnetic hour angle from the midnight meridian, calculated from the above maps (correspondence indicated by the letters *a*–*h*). The location where the sunlight terminator crosses the peak current is indicated by dashed vertical lines.

the sunlight terminator, contribute significantly to asymmetries in auroral intensity.

## 10.3. SUMMARY

In this chapter we have reviewed some new results on nonconjugate phenomena that have been reported the last couple of years. We have focused on the three suggested mechanisms to produce asymmetric aurora in the conjugate hemispheres. The results can be summarized as follows:

1. There are statistically significant brightness differences in the duskside aurora in the poleward part of the oval, when IMF has a $B_x$ component of >2 nT. The differences are consistent with stronger region 1 currents that flow out of the duskside ionosphere, which is expected from a more efficient solar wind dynamo due to an IMF $B_x$ component.

2. IMF $B_y$ does, indeed, lead to asymmetric footpoints of closed field lines. This has been shown by in situ measurements and many studies on asymmetric auroral substorm onset locations. However, the IMF $B_y$ does not penetrate the closed magnetosphere but induces a $B_y$ component with the same polarity as IMF. We have discussed the current systems that should be expected from this $B_y$ component. We have revised our earlier view and

suggest that they are not interhemispheric currents, but instead pairs of balanced FAC systems transmitting the asymmetric magnetic stress from the magnetospheric sources to each ionosphere.

3. Interhemispheric currents due to conductivity differences have been estimated by models to be of similar strength as region 1 and region 2 currents. Statistical results based on AMPERE data do not support the existence of currents in the vicinity of the terminator with such magnitudes.

## ACKNOWLEDGMENTS

This study was supported by the Research Council of Norway/CoE under contract 223252/F50. S. E. Milan received support from the Science and Technology Facilities Council (UK), Grant ST/K001000/1. We thank the AMPERE team and the AMPERE Science Center for providing the Iridium-derived data products.

This manuscript was prepared with AGU's $L^{A}T_{E}X$ macros v5, with the extension package 'AGU$^{++}$' by P. W. Daly, version 1.6b from 1999/08/19.

## REFERENCES

Anderson, B. J., H. Korth, C. L. Waters, D. L. Green, and P. Stauning (2008), Statistical Birkeland current distributions from magnetic field observations by the Iridium constellation, *Ann. Geophys.*, *26*, 671–687.

Belon, A. E., J. E. Maggs, T. N. Davis, K. B. Mather, N. W. Glass, and G. F. Hughes (1969), Conjugacy of visual auroras during magnetically quiet periods, *J. Geophys. Res.*, *74*, 1–28.

Benkevich, L., W. Lyatsky, and L. L. Cogger (2000). Field-aligned currents between conjugate hemispheres, *J. Geophys. Res.*, *102*, 27,727–27,737.

Bobra, M. G., S. M. Petrinec, S. A. Fuselier, S. S. Claflin, and H. E. Spence (2004), On the solar wind control of cusp aurora during northward IMF, *Geophys. Res. Lett.*, *31*, L04805, doi:10.1029/2003GL018417.

Burns, G. B., D. J. McEwen, R. A. Eather, F. T. Berkey, and J. S. Murphree (1990), Optical auroral conjugacy: Viking UV imager—South Pole station ground data, *J. Geophys. Res.*, *95*, 5781–5790.

Cowley, S. W. H. (1981a), Magnetospheric asymmetries associated with the Y-component of the IMF, *Planet. Space Sci.*, *29*, 79–96.

Cowley, S. W. H., (1981b), Asymmetry effects associated with the X-component of the IMF in a magnettically open magnetosphere, *Planet. Space Sci.*, *29*, 809–818.

Craven, J. D., J. S. Murphree, L. A. Frank, and L. L. Cogger (1991), Simultaneous optical observations of transpolar arcs in the two polar caps, *Geophys. Res. Lett.*, *18*, 2297–2300.

Dungey, J. W. (1961), Interplanetary magnetic field and the auroral zones, *Phys. Rev. Lett.*, *6*, 47–48.

Frank, L. A., and J. B. Sigwarth (2003), Simultaneous images of the northern and southern auroras from the Polar spacecraft: An auroral substorm, *J. Geophys. Res.*, *108*, 8015, doi:10.1029/2002JA009356.

Frank, L. A., J. B. Sigwarth, J. D. Craven, J. P. Cravens, J. S. Dolan, M. R. Dvorsky, P. K. Hardebeck, J. D. Harvey, and D. W. Muller (1995), The visible imaging system (VIS) for the Polar spacecraft, *Space Sci. Rev.*, *71*, 297–328.

Green, D. L., C. L. Waters, B. J. Anderson, and H. Korth (2009), Seasonal and interplanetary magnetic field dependence of the field-aligned currents for both Northern and Southern Hemispheres, *Ann. Geophys.*, *27*, 1701–1715.

Hargreaves, J. K., and H. J. A. Chivers (1964), Fluctuations in ionospheric absorption events at conjugate stations, *Nature*, *203*, 963–964.

Khurana, K. K., R. J. Walker, and T. Ogino (1996), Magnetospheric convection in the presence of interplanetary magnetic *By* : A conceptual model and simulations, *J. Geophys. Res.*, *101* (A3), 4907–4916.

Laundal, K. M., and N. Østgaard (2009), Asymmetric auroral intensities in the Earth's Northern and Southern hemispheres, *Nature*, *460*, 491–493.

Laundal, K. M., N. Østgaard, K. Snekvik, and H. U. Frey (2010a), Inter-hemispheric observations of emerging polar cap asymmetries, *J. Geophys. Res.*, *115* (A7), A07,230, doi: 10.1029/2009JA015160.

Laundal, K. M., N. Østgaard, H. U. Frey, and J. M. Weygand (2010b), Seasonal and interplanetary magnetic field-dependent polar cap contraction during substorm expansion phase, *J. Geophys. Res.*, *115* (A11), A11,224, doi:10.1029/2010JA015910.

Liou, K., and P. T. Newell (2010), On the azimuthal location of auroral breakup: Hemispheric asymmetry, *Geophys. Res. Lett.*, *37* (L23103), doi:10.1029/2010GL045537.

Liou, K., P. T. Newell, and C. I. Meng (2001a), Seasonal effects on auroral particle acceleration and precipitation, *J. Geophys. Res.*, *106*, 5531–5542.

Liou, K., P. T. Newell, D. G. Sibeck, C. I. Meng, M. Brittnacher, and G. Parks (2001b), Observation of IMF and seasonal effects in the location of auroral substorm onset, *J. Geophys. Res.*, *106*, 5799–5810.

Lyatskaya, S., W. Lyatsky, and G. V. Khazanov (2008), Relationship between substorm activity and magnetic disturbances in two polar caps, *Geophys. Res. Lett.*, *35*, L20104, doi:10.1029/2008GL035187.

Lyatskaya, S., G. V. Khazanov, and E. Zesta (2014), Interhemispheric field-aligned currents: Simulation results, *J. Geophys. Res.*, *119*, doi:10.1002/2013JA019558.

Mende, S. B. et al. (2000), Far ultraviolet imaging from the IMAGE spacecraft. 3. Spectral imaging of Lyman-$\alpha$ and OI 135.6 nm, *Space Sci. Rev.*, *91*, 287–318.

Meng, C. I., K. Liou, and P. T. Newell (2001), Asymmetric sunlight effect on dayside/nightside auroral precipitation, *Phys. Chem. Earth Part C*, *26*, 43–47.

Motoba, T., K. Hosokawa, N. Sato, A. Kadokura, and G. Bjornsson (2010), Varying interplanetary magnetic field by effects on interhemispheric conjugate auroral features during a weak substorm, *J. Geophys. Res.*, *115* (A09210), doi:10.1029/2010JA015369.

Newell, P. T., K. M. Lyons, and C.-I. Meng (1996), A large survey of electron acceleration events, *J. Geophys. Res.*, *101*, 2559–2614.

Newell, P. T., T. Sotirelis, and S. Wing (2010), Seasonal variations in diffuse, monoenergetic, and broadband aurora, *J. Geophys. Res.*, *115*, doi:10.1029/2009JA014805.

Ohtani, S.-I., G. Ueono, T. Higuchi, and H. Kawano (2005), Annual and semiannual variations of the location and intensity of large-scale field-aligned currents, *J. Geophys. Res.*, *110* (A1), A01216, doi:10.1029/2004JA010634.

Olsen, N. (1997), Ionospheric F region currents at middle and low latitudes estimated from Magsat data, *J. Geophys. Res.*, *102*, 4563–4576.

Østgaard, N., and K. M. Laundal (2012), Auroral asymmetries in the conjugate hemispheres and interhemispheric currents, in A. Keiling, E. Donovan, F. Bagenal, and T. Karlsson (eds.), *Auroral Phenomenology and Magnetospheric Processes*, Geophys. Monograph Series Vol. *197*, Washington, DC: American Physical Union (AGU).

Østgaard, N., S. B. Mende, H. U. Frey, L. A. Frank, and J. B. Sigwarth (2003), Observations of non-conjugate theta aurora, *Geophys. Res. Lett.*, *30* (21), 2125. 2.

Østgaard, N., S. B. Mende, H. U. Frey, T. J. Immel, L. A. Frank, J. B. Sigwarth, and T. J. Stubbs (2004), Interplanetary magnetic field control of the location of substorm onset and auroral features in the conjugate hemispheres, *J. Geophys. Res.*, *109* (A7), A07204, doi:10.1029/2003JA010370.

Østgaard, N., S. B. Mende, H. U. Frey, and J. B. Sigwarth (2005a), Simultaneous imaging of the reconnection spot in the opposite hemispheres during northward IMF, *Geophys. Res. Lett.*, *32* (5), L21104, doi:10.1029/2005GL024491.

Østgaard, N., N. A. Tsyganenko, S. B. Mende, H. U. Frey, T. J. Immel, M. Fillingim, L. A. Frank, and J. B. Sigwarth (2005b), Observations and model predictions of auroral substorm asymmetries in the conjugate hemispheres, *Geophys. Res. Lett.*, *32* (5), L05111, doi:10.1029/2004GL022166.

Østgaard, N., S. B. Mende, H. U. Frey, J. B. Sigwarth, A. Aasnes, and J. M. Weygand (2007), Auroral conjugacy studies based on global imaging, *J. Atmosph. Sol. Terr. Phys.*, *69*, 249–255.

Østgaard, N., B. K. Humberset, and K. M. Laundal (2011a), Evolution of auroral asymmetries in the conjugate hemispheres during two substorms, *Geophys. Res. Lett.*, *38*, L03101, doi:10.1029/2010GL046057.

Østgaard, N., K. M. Laundal, L. Juusola, A. Åsnes, S. E. Håland, and J. M. Weygand (2011b), Interhemispherical asymmetry of substorm onset locations and the interplanetary magnetic field, *Geophys. Res. Lett.*, *38*, L08104, doi:10.1029/2011GL046767.

Reistad, J. P., N. Østgaard, K. M. Laundal, and K. Oksavik (2013), On the non-conjugacy of nightside aurora and their generator mechanisms, *J. Geophys. Res.*, *118*, doi:10.1002/jgra.50300.

Reistad, J. P., N. Østgaard, K. M. Laundal, S. Haaland, P. Tenfjord, K. Snekvik, K. Oksavik, and S. E. Milan (2014), Hemispheric asymmetries in solar wind dynamo efficiency due to IMF *Bx*, *J. Geophys. Res.*, *119*, doi:10.1002/2014JA020216.

Richmond, A. D., and R. G. Roble (1987), Electrodynanic effects of thermospheric winds from the NCAR thermospheric general circulation model, *J. Geophys. Res.*, *92*, 12,365–12,376.

Sandholt, P. E., and C. J. Farrugia (1999), On the dynamic cusp aurora and IMF *By* , *J. Geophys. Res.*, *104*, 12,461–12,472.

Sandholt, P. E., C. J. Farrugia, J. Moen, O. Noraberg, B. Lybekk, T. Sten, and T. Hansen (1998), A classification of dayside auroral forms and activities as a function of interplanetary magnetic field orientation, *J. Geophys. Res.*, *103*, 23,325–23,345.

Sato, N., R. Fujii, T. Ono, H. Fukunishi, T. Hirasawa, T. Araki, S. Kokubun, K. Makita, and T. Saemundsson (1966), Conjugacy of proton and electron auroras observed near L=6.1, *Geophys. Res. Lett.*, *13*, 1368–1371.

Sato, N., T. Nagaoka, K. Hashimoto, and T. Saemundsson (1998), Conjugacy of isolated auroral arcs and non-conjugate auroral break-ups, *J. Geophys. Res.*, *103*, 11,641–11,652.

Shue, J.-H., P. T. Newell, K. Liou, and C.-I. Meng (2001), Influence of interplanatery magnetic field on global auroral patterns, *J. Geophys. Res.*, *106*, 5913–5926.

Shue, J.-H., P. T. Newell, K. Liou, and C.-I. Meng (2002), Interplanetary magnetic field *By* asymmetry effect on auroral brightness, *J. Geophys. Res.*, *107* (1197), doi:10.1029/2001JA000229.

Stenbaek-Nielsen, H. C., and A. Otto (1997), Conjugate auroras and the interplanetary magnetic field, *J. Geophys. Res.*, *102*, 2223–2232.

Stenbaek-Nielsen, H. C., T. N. Davis, and N. W. Glass (1972), Relative motion of auroral conjugate points during substorms, *J. Geophys. Res.*, *77*, 1844–1852.

Stenbaek-Nielsen, H. C., E. M. Wescott, T. N. Davis, and R. W. Peterson (1973), Auroral intensity differences at conjugate points, *J. Geophys. Res.*, *78*, 659–671.

Tenfjord, P., N. Østgaard, J. P. Reistad, K. M. Laundal, S. Haaland, K. Snekvik, and S. E. Milan (2015), The impact of IMF *By* on the magnetosphere-ionopshere coupling, *J. Geophys. Res.*, in press, doi:10.1029/2015JA021579.

Vorobjev, V. G., O. I. Yagodkina, D. Sibeck, K. Liou, and C. I. Meng (2001), Aurora conjugacy during substorms: Coordinated Antarctic ground and Polar Ultraviolet observations, *J. Geophys. Res.*, *106*, 24,579–24,591.

Wang, H., H. Luöhr, S. Y. Ma, and H. U. Frey (2007), Interhemispheric comparison of average substorm onset locations: evidence for deviation from conjugacy, *Ann. Geophys.*, *25*, 989–999.

Wing, S., S.-I. Ohtani, P. T. Newell, T. Higuchi, G. Ueno, and J. M. Weygand (2010), Dayside field-aligned current source regions, *J. Geophys. Res.*, *115*, doi:10.1029/2010JA015837.

Zhou, X.-W., C. T. Russell, and G. Le (2000), Local time and interplanetary magnetic field *By* dependence of field-aligned currents at high altitudes, *J. Geophys. Res.*, *105*, 25,533–25,539.